Dartmouth College

Dartmouth Digital Commons

Stellar Pollution in the Solar Neighborhood

N. Murray
University of Toronto

B. Chaboyer
Dartmouth College

P. Arras
University of Toronto

B. Hansen
University of Toronto

R. W. Noyes
4 Harvard-Smithsonian Center for Astrophysics

Follow this and additional works at: https://digitalcommons.dartmouth.edu/facoa

Part of the Stars, Interstellar Medium and the Galaxy Commons, and the The Sun and the Solar System Commons

STELLAR POLLUTION IN THE SOLAR NEIGHBORHOOD

N. MURRAY,[1] B. CHABOYER,[2] P. ARRAS,[1] B. HANSEN,[1,3] AND R. W. NOYES[4]

ABSTRACT

We study spectroscopically determined iron abundances of 640 solar-type stars to search for the signature of accreted iron-rich material. We find that the metallicity [Fe/H] of a subset of 466 main-sequence stars, when plotted as a function of stellar mass, mimics the pattern seen in lithium abundances in open clusters. Using Monte Carlo models, we find that, on average, these stars appear to have accreted ~ 0.5 $M_\oplus$ of iron while on the main-sequence. A consistency check is provided by a much smaller sample of 19 stars in the Hertzsprung gap, which are slightly evolved and the convection zones of which are significantly more massive; they have lower average [Fe/H], and their metallicity shows no clear variation with stellar mass. We argue that our Sun is likely to have accreted a similar amount of iron; in this respect, most systems resemble ours rather than the currently known extrasolar planetary systems. These findings suggest that terrestrial-type material is common around solar-type stars.

Subject headings: accretion, accretion disks — planetary systems — stars: abundances — stars: chemically peculiar

1. INTRODUCTION

The fraction of main-sequence stars harboring terrestrial planets is currently almost completely unconstrained by observation. Earth is not unique since there are three other terrestrial bodies in our solar system and three more orbiting the pulsar PSR 1257+12 (Wolszczan & Frail 1992). How many stars are orbited by terrestrial planets?

The discovery that at least 6%–8% of solar-type stars harbor Jupiter-mass or larger bodies, often in small, eccentric orbits (Mayor & Queloz 1995; Marcy & Butler 1996; Butler & Marcy 1996; Marcy, Cochran, & Mayor 2000) shows that Jupiter-mass planets are not exceptionally rare. The transiting planet orbiting HD 209458 has a mass of 0.69 Jupiter masses and a radius about 1.4 times that of Jupiter. Clearly it is a gas giant like Jupiter or Saturn; the minimum masses of the other known objects suggest that they are also gas giants. The Doppler technique used for most of the discoveries cannot find terrestrial mass objects in AU scale orbits. What fraction of solar-type stars have terrestrial-type planets?

How could an observer with our current technology located on a star in the solar neighborhood decide if there were any terrestrial-type bodies orbiting the Sun? More generally, how could such an observer estimate the fraction of solar-type stars having companions of terrestrial (as opposed to gas giant) compositions? This paper explores one possible way of addressing the latter question, stellar-mass dependent photospheric metallicity trends.

The work reported in this paper is motivated by the Copernican assumption that our solar system is not unusual; there are likely to be other stars in the neighborhood of the Sun that are orbited by both terrestrial and gas

giant planets. We explicitly argue in this paper that most systems are like ours rather than like the currently known extrasolar planetary systems; the clearest evidence for this is the extreme iron abundances seen in the latter (Laughlin 2001; Santos, Israelian, & Mayor 2000; Murray et al. 2001). In § 2 we argue that a few Earth masses of rocky/icy material have accreted onto the Sun over its lifetime. Section 3 discusses one possible observational tracer of similar accretion occurring on other solar-type stars. In § 4, we examine a sample of stars with spectroscopically measured photospheric iron abundances

$$\left[\frac{\text{Fe}}{\text{H}}\right] \equiv \log\left[\frac{f_{\text{Fe}}}{f_{\text{Fe},\odot}}\right], \qquad (1)$$

where f_{Fe} is the mass abundance of iron in the photosphere of the star, and $f_{\text{Fe},\odot} \approx 1.3 \times 10^{-3}$ is the mass abundance of iron in the photosphere of the Sun. We compare the observations to Monte Carlo models of stellar pollution in § 5. We discuss the implications of our results in § 6 and present our conclusions in the final section. In a companion paper (Murray et al. 2001), we discuss evidence that the host stars in the recently discovered extrasolar planetary systems are *not* like most stars; they have accreted much more iron (see also Laughlin 2001; Santos et al. 2000).

2. POLLUTION BY SMALL BODIES IN OUR SOLAR SYSTEM

The surface density Σ_{Fe} of iron in our solar system follows a rough power law with distance from the Sun (Weidenschilling 1977). We have compiled recent estimates for the iron content of the planets in Table 1. From a least-squares fit including Venus, Earth, and the four gas giants, we find $\Sigma_{\text{Fe}} \sim 4(r/1 \text{ AU})^{-1.7}$ g cm^{-2}. Weidenschilling noted a clear deficit of material in the region interior to Venus, and between Earth and Jupiter, relative to this power law. Gas drag acting on planetesimals near the Sun could reduce the surface density of such bodies near the present orbit of Mercury by dropping them onto the Sun. Because the solar convection zone was very deep for ~ 20 million years (see Fig. 1), while the gas disk that would have produced the drag is believed to have survived only a few million, this would not have altered the apparent metallicity of the Sun.

[1] Canadian Institute for Theoretical Astrophysics, 60 St. George Street, University of Toronto, Toronto, ON M5S 3H8, Canada; murray@cita.utoronto.ca, arras@cita.utoronto.ca.

[2] Department of Physics and Astronomy, Dartmouth College, 6127 Wilder Laboratory, Hanover, NH 03755-3528; chaboyer@heather.dartmouth.edu.

[3] Present address: Department of Astrophysical Sciences, Princeton University, Princeton, NJ 08544-1001; hansen@astro.princeton.edu.

[4] Harvard-Smithsonian Center for Astrophysics, 60 Garden Street, Cambridge, MA 02138; noyes@cfa.harvard.edu.

Planet	$M_{Fe}/M_{\oplus}$	Zone Boundaries (AU)	Σ_{Fe} (g cm^{-2})
Mercury	3.3×10^{-2}	0.22–0.56	1.1
Venus	0.29	0.56–0.86	5.7
Earth	0.38	0.86–1.26	4.0
Mars	0.03	1.26–2.0	0.11
Asteroids......	0.0005	2.0–3.3	6.2×10^{-4}
Jupiter	1.8	3.3–7.4	0.36
Saturn.........	1.7	7.4–14.4	0.11
Uranus........	0.9	14.4–24.7	0.019
Neptune	1.0	24.7–35.5	0.013

NOTE.—Data for Mercury, Venus, Earth, and the asteroids are from
Weidenschilling 1977; for Mars from Longhi et al. 1992; for Jupiter
and Saturn from Guillot 1999b; for Uranus from Podolak et al. 1991;
for Neptune from Hubbard et al. 1995. For the gas giants, we take
representative values for the heavy-element mass; the typical uncer-
tainty is roughly ±30%. The zone boundaries are those of Weiden-
schilling. Using these values, and assuming solar abundances, we find
the iron masses given in the table.

Material in the asteroid belt clearly survived such gas
drag. However, Kirkwood noticed over one hundred years
ago that the distribution of asteroids showed distinct gaps
at the location of orbital resonances with Jupiter
(Kirkwood 1867). This suggests that material has been
removed from the gaps under the influence of Jupiter. Over
the last twenty years, the dynamics of this removal have
been worked out in considerable detail (Wisdom 1983;
Holman & Murray 1996; Gladman et al. 1997). The gaps
are the result of resonant, chaotic perturbations of the aster-

oid orbits by Jupiter. A second feature, seen in plots of
orbital eccentricity versus semimajor axis, is the result of a
secular resonance, the ν_6 resonance. In either type of reso-
nance, bodies with semimajor axis larger than about half
that of Jupiter's tend to be removed from the solar system;
their eccentricities grow with time, increasing their apo-
apses until they reach the orbit of Jupiter. Close encounters
with that planet then quickly eject the asteroids.

Resonant asteroids in smaller orbits tend not to be
ejected; their apoapse does not reach the orbit of Jupiter.
Instead, their periapses decrease until they hit the Sun.
Several related mechanisms can combine to produce this
decrease in periapse, but the two main actors are mean
motion resonances and the ν_6 resonance already men-
tioned. In a mean motion resonance such as that
responsible for the 3/1 Kirkwood gap, the eccentricity of the
resonant asteroid undergoes a random walk. Since the
eccentricity cannot decrease below zero, there is a tendency
for bodies with small e to drift to larger e. When the eccen-
tricity is large enough, the asteroid strikes the Sun
(Gladman et al. 1997). A small fraction will suffer close
encounters with the Earth or other terrestrial bodies; this
may lead to Jupiter crossing orbits, which usually leads to
ejection of the asteroid from the solar system. Only a very
small fraction will collide with either a terrestrial planet or
Jupiter. In the ν_6 secular resonance, the precession rate
equals the sixth secular frequency of the solar system. This
frequency appears with substantial amplitude in the orbital
motion of both Jupiter and Saturn; it is roughly the average
precession rate of the latter planet. The ν_6 resonance rapidly
removes angular momentum from the orbit of the asteroid,
dropping the periapse below the surface of the Sun.

These resonances are currently active and are believed to
be responsible for the bulk of the meteorites striking the
Earth. While there is no direct observational confirmation,
it is virtually certain that a much larger flux of asteroidal
material from these resonances is currently hitting the Sun.

It is also likely that the flux of asteroidal material was
much larger in the past. The location of both mean motion
and secular resonances depends on the positions of Jupiter
and Saturn and on any massive gas disk. It has been sug-
gested that as the protoplanetary gas disk dissipated, the ν_6
resonance swept through the belt, depleting much of the
mass. More recently it has been suggested that one or both
of Jupiter and Saturn migrated to their current positions,
causing a similar sweeping of mean motion resonances. This
would preferentially deplete the outer belt (Holman &
Murray 1996; Liou & Malhotra 1997) but would also drop
material from the inner belt onto the Sun. Finally, we note
that the asteroid belt is hot, in the sense that the distribu-
tion of both e and i is broad. A number of authors have
suggested that a planet-sized body swept through the region
early in the history of the solar system, heating the belt as
well as dropping material on the star (Wetherill 1992; Petit
et al. 1991).

The surfaces of the terrestrial planets and the Moon show
evidence for an extended period of bombardment, known as
the late heavy bombardment, lasting up to a billion years
after their surfaces cooled. This is consistent with some of
the longer lived depletion scenarios described above.

From Table 1, the amount of material inferred to have
populated the original asteroid belt is of order 5 to 10 Earth
masses. Roughly 2–5 Earth masses would have been
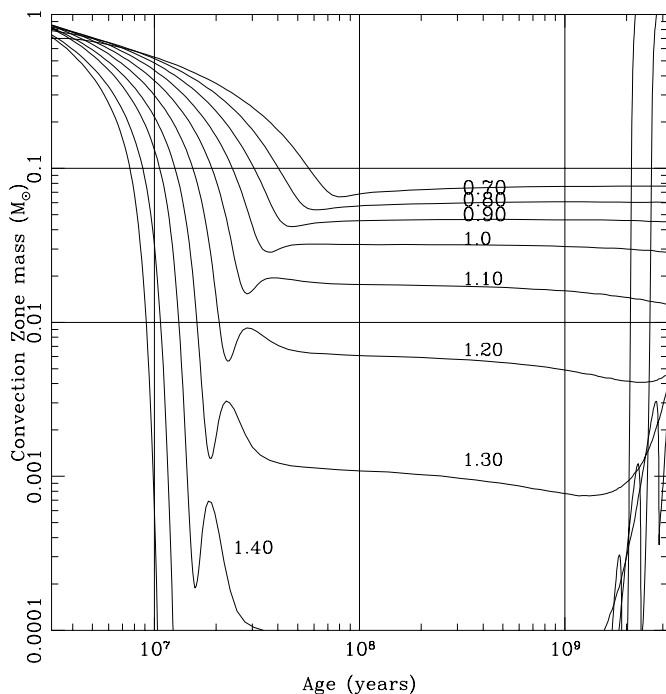between the present position of Mars and 2.5 AU, half the

FIG. 1.—Mass of the convection zone for solar metallicity ([Fe/H] = 0)
stars, plotted as a function of stellar age. The stellar mass is used to label
the curves. Note that for ages less than about 7 million yr, all stars in the
mass range 0.6–1.6 $M_{\odot}$ have convection zone masses greater than 0.1 $M_{\odot}$;
stars this young have not yet reached the main sequence. The Yale stellar
evolution code was used to calculate the masses (see § 4).

present semimajor axis of Jupiter. A substantial fraction of this material, of order half, would have ended up in the Sun. We will take $\sim 2\ M_\oplus$ as a representative number. Meteoritic material is roughly 20% iron by weight (Grevesse & Anders 1989), so we take $\sim 0.5\ M_\oplus$ as the amount of iron that was dropped on the Sun after the convection zone thinned. Taking the Copernican viewpoint, we expect that a typical star in the solar neighborhood has accreted a similar amount of iron over the first billion or so years of its existence.

3. POSSIBLE OBSERVATIONAL EVIDENCE FOR POLLUTION

There is another possible piece of evidence besides the late heavy bombardment for such a late depletion of the asteroid belt. As we noted above, a substantial fraction of the "missing" material originally in the asteroid belt strikes the Sun. This material will be mixed throughout the convection zone of the star. Since a substantial bombardment of the terrestrial planets lasted for much longer than 100 million years, this material would have landed in a convection zone of mass $\sim 3 \times 10^{-2}\ M_\odot$. Hence, there is a possibility that the signature of solar bombardment was left in the form of an enhanced metallicity in the solar envelope.

The mass of the convection zone was $\sim 3\%$ of the solar mass between 10^8 and 10^9 yr, while the present mass fraction of iron observed in the photosphere is 1.3×10^{-3}. This yields a total iron content of $\sim 12.75\ M_\oplus$ between 10^8 and 10^9 yr. Adding half an Earth mass of iron would increase the observed [Fe/H] by only ≈ 0.017 dex.

Precision measurements of the bulk metallicity of a single solar-type star are not available at present. Measurements of the sound speed in the interior of the Sun, using the 5 minute oscillations, could in principle provide such a measurement. The only work along these lines that we are aware of is the paper by Henney & Ulrich (1998). They show that the addition of $\sim 8\ M_\oplus$ of cometary material results in a frequency shift that, because of uncertainties in solar models, is too small to be detected.

However, it is possible that observations of large numbers of stars could reveal the presence of pollution. For example, stars having a fixed metallicity but different masses will mix material dropped onto their surfaces to different depths. Knowledge of the depth of this surface mixing layer, which we summarize in the next subsection, allows us to look for variations of metallicity with stellar mass produced by accreted material.

3.1. The Mass of the Surface Mixing Region

Material dropped onto the surface of a star will not in general be confined to the photosphere. The surface layers of stars less than about $1.4\ M_\odot$ are convectively unstable, and any material dropped on the star is expected be mixed throughout the convection zone. Observations of lithium (Li) abundance provide support for this theoretical picture. But these same observations suggest that there is another form of mixing in stars more massive than $\sim 1.2\ M_\odot$, possibly related to stellar rotation.

The evidence for the two types of mixing comes in the form of variations in the surface lithium abundance with stellar mass. Lithium is destroyed when it is exposed to temperatures above about 3.1×10^6 K; the temperature at the photosphere is much lower than this, so lithium depletion indicates that photospheric material is mixed down to regions where the temperature is higher. Lithium could also

be removed from the photosphere by simple settling (so that the lithium is stored below the photosphere as opposed to being destroyed) or by stellar mass loss. However, the observations, which we review below, point to destruction by mixing.

Observations show that for stars with mass below $\sim 1.2\ M_\odot$ the photospheric abundance of lithium decreases rapidly with decreasing stellar mass (e.g., Boesgaard 1991). Some depletion occurs before the main sequence, but there is strong evidence that depletion also occurs on the main sequence (Jones et al. 1999). The main-sequence depletion is believed to be related to the increasing depth of the bottom of the surface convection zone with decreasing stellar mass in these stars, supplemented by some convective overshoot and/or settling in stars near the upper end of this mass range.

Stars above about $1.2\ M_\odot$ have very thin, or even nonexistent, convection zones. In standard stellar models, with no settling, mixing or mass loss, the surface Li and Be abundances are constant over the main-sequence lifetime of such high-mass stars. Both Li and Be are destroyed below modest depths in the interiors of such stars. For stars in the mass range 1.2–1.6 $M_\odot$ and having solar metallicity, our stellar models indicate that the nominally undepleted region has a mass of $\gtrsim 3 \times 10^{-2}\ M_\odot$ for Li and $\gtrsim 6 \times 10^{-2}\ M_\odot$ for Be. At depths below those corresponding to these masses, Li and Be should be destroyed.

Real stars with masses larger than $1.2\ M_\odot$ do not behave like the models. Hyades stars show a distinct "lithium dip" centered at 1.4 $M_\odot$ (Boesgaard & Tripicco 1986). Between ~ 1.2 and 1.4 $M_\odot$ the lithium abundance is seen to decrease with increasing stellar mass. From 1.4 to 1.5 $M_\odot$ there is a sharp increase in lithium abundance. Balachandran (1995) finds the highest abundances for stars with masses above 1.5 $M_\odot$ (the "blue side" of the dip) and for stars of $\approx 1.2\ M_\odot$ (the "red side" of the dip); these stars have abundances about equal to those found in meteorites (Grevesse & Anders 1989), abundances which are generally believed to be primordial.

Observations of young stellar clusters such as α Per and the Pleiades find little evidence of lithium depletion in more massive stars (Soderblom et al. 1993). Indeed, there is a strong correlation between cluster age and Li abundance in the "lithium dip" between 1.2 and 1.5 $M_\odot$, indicating that the depletion takes place on the main sequence on a timescale of 100 Myr or more (Boesgaard 1991).

Observations of clusters having different metallicities [Fe/H] show that the location of the dip is slightly metallicity dependent (Balachandran 1995). Lower metallicity clusters have dips centered at lower masses. However, the high-mass side of the dip depends only weakly on metallicity.

The lithium depletion seen in stars above 1.2 $M_\odot$ cannot be caused by convective mixing since the convection is either shallow or nonexistent. Nor is this depletion caused by either gravitational settling or stellar mass loss. Two observations lead to this conclusion. First, surface depletions of lithium and beryllium are correlated, with the surface lithium diminishing more rapidly than surface beryllium (Deliyannis et al. 1998). Because the Be rich zone has twice the mass of the Li rich zone, mass loss would deplete all the Li before depleting the surface Be. Similarly, settling predicts that surface Li and Be would be depleted at roughly the same rate. Second, evolved stars with

1.2 < M < 1.5 are also deficient in lithium (Gilroy 1989; Balachandran 1995); settling of lithium would leave a non-depleted layer of lithium below the surface (in the absence of mixing), which would be dredged up to the surface when the convection zone deepens. The fact that the predicted increase in evolved stars is not seen indicates that the Li missing from main-sequence stellar photospheres is destroyed rather than sequestered below the photosphere.

Thus, there seems to be an additional source of surface mixing in stars with masses between 1.2 and 1.5 $M_\odot$, which mixes their surface lithium down to regions with temperatures of order 3×10^6 K. The surface mixing seen in the dip appears to be rotationally induced (Charbonnel, Vauclair, & Zahn 1992; Balachandran 1995; Talon & Charbonnel 1998), although this is far from certain.

As already noted, stars in α Per and the Pleiades clusters, with estimated ages of 50 and 70 million years, show little depletion in Li abundance for stars between 1.2 and 1.5 $M_\odot$, while stars in the Hyades and older clusters show depletions that increase with cluster age. We interpret this to mean that the upper layers of the stars are mixed downward on timescales of ~ 100 million years.

Above 1.5 $M_\odot$ there appears to be little mixing of the upper layers of the star with deeper layers since there is little Li depletion. However, the lithium in these stars does appear to be destroyed in deeper layers; evolved (giant) 1.6 $M_\odot$ stars are severely depleted (Gilroy 1989). This depletion occurs inside the progenitors, below the photosphere (Vauclair 1991), so that when the surface convection zone forms and then thickens, the surface lithium is mixed over a larger volume of depleted material, reducing the photospheric lithium abundance.

The observational data summarized here leads us to propose the following simple model for the mass M_{mix} of the surface mixing region in solar mass stars (see Fig. 2). We first describe the lithium dip. The location, in mass, of the dip is described by M_{red}, $M_{central}$, and M_{blue}, giving the low, central, and high mass points of the dip. These three masses depend on the stellar [Fe/H].

Extrapolating from data in (Balachandran 1995), we take

$$M_{blue}/M_\odot = 1.52 + 0.054[Fe/H] , \qquad (2)$$

$$M_{central}/M_\odot = 1.45 + 0.15[Fe/H] , \qquad (3)$$

$$M_{red}/M_\odot = 1.1 + 0.31[Fe/H] . \qquad (4)$$

Note that the high mass or blue side of the dip is essentially independent of [Fe/H].

As for the mass M_{mix} of the surface mixing region, we proceed in two steps. First we use a piecewise linear model for the mass M_{non} of the surface mixing layer produced by nonconvective means. We then add to this mass the mass of the convection zone to arrive at $M_{mix} = M_{cvz} + M_{non}$; adding the two masses ensures that M_{mix} is continuous and gives the appropriate limits for both low and high stellar masses.

For stellar masses M_* above M_{blue} (where the mass of the convection zone is zero) we assume $M_{non} = M_{mb}$, where the subscript "m" refers to mixing and "b" refers to the blue or high mass side of the dip. The minimum value of M_{mb} is currently unconstrained by observation, but its maximum value must be less than $\approx 5 \times 10^{-3} M_\odot$ to prevent Li depletion. Models of meridional circulation suggest masses of order $3 \times 10^{-3} M_\odot$. We examine models with both these values. At the center of the dip, M_{non} is taken to be $M_{mc} = 2$
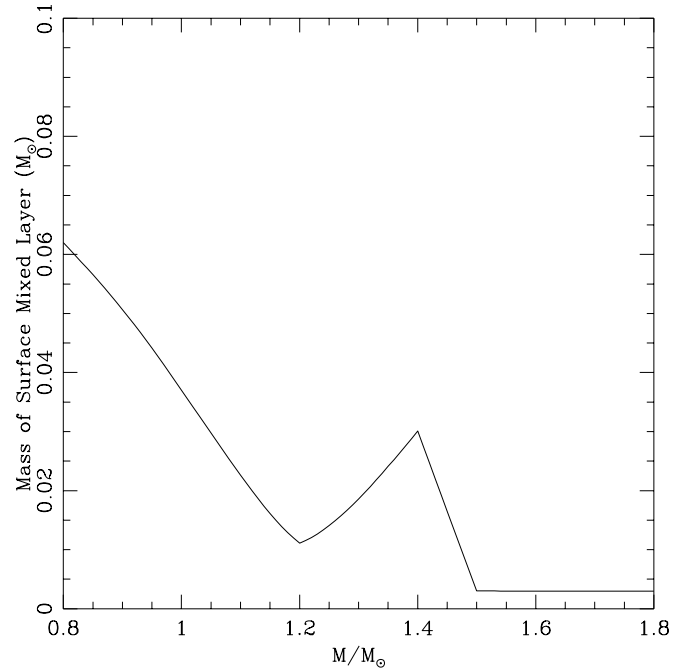

FIG. 2.—Mass of the surface mixing layer of solar metallicity stars. For masses below about 1.0 $M_\odot$, the mass is assumed to be the mass of the convection zone, as calculated in our stellar models. Above 1.5 $M_\odot$, the mass is assumed to be $3 \times 10^{-3} M_\odot$, as predicted by meridional circulation models. Between these masses, the mixed region is chosen by comparison to observations of the lithium dip. See the text for a more detailed explanation.

$\times 10^{-2} M_\odot$, which allows for complete Li depletion but only partial Be depletion. For $M_{central} \le M_* < M_{blue}$, we use a linear interpolation between M_{mb} and M_{mc}.

On the low-mass side of the dip, below M_{red}, we take $M_{non} = M_{mr} = 7 \times 10^{-3}$ since stars at the low-mass edge of the dip are typically slightly more depleted in Li than stars at the high-mass edge. Between M_{red} and $M_{central}$ we use a linear interpolation between M_{mr} and M_{mc} to find M_{non}.

To complete our empirical estimate for M_{mix}, we need the mass M_{cvz} of the surface convection zone. The mass of the convection zone at an age of 10^8 yr (the mass at 10^9 is similar—see Fig. 1) is found from the following empirical fit, derived from our stellar models:

$$M_{cvz} = a([Fe/H]) \times (M_{-3} - M_*)^{3.65} , \qquad (5)$$

where $a([Fe/H]) = -0.2[Fe/H] + 0.49$. The quantity M_{-3} is the (metallicity-dependent) stellar mass at which the convection zone mass equals $10^{-3} M_\odot$,

$$M_{-3} = a_{-3}[Fe/H] + b_{-3} , \qquad (6)$$

where $a_{-3} = 0.32$ and $b_{-3} = 1.45$. Equation (5) is very accurate near M_{-3} and good to about 20% at 0.8 $M_\odot$.

Our model for the depth of the mixing region in a solar metallicity star is shown in Figure 2; this example has $M_{mb} = 3 \times 10^{-3} M_\odot$. Note that stars of different metallicity will have "lithium dips" (peaks in this figure) at slightly different masses than those shown in the figure. Furthermore, stars of a given mass and metallicity show a range of lithium abundances (Balachandran 1995) from nearly totally depleted to only marginally depleted, indicating that there is a third parameter influencing the depth of the mixing region. This could be modeled by varying M_{mb},

M_{mc}, and M_{mr} and would have the effect of decreasing M_{mc}; in the models explored here, we have not accounted for this effect. We stress that our model is only a very rough empirical attempt to mimic the observed Li abundance trends. It has the virtues that it is simple to evaluate and that, once it has been derived from the Li data, it has only one free parameter (M_{mb}) as far as comparisons with the iron data are concerned.

Armed with this model, we can predict the average change in metallicity of a sample of stars subjected to iron accretion. Essentially we will look for behavior similar to that seen in the abundance of lithium. Polluted low-mass stars of a fixed age will show an increase in metallicity with increasing mass (below the low-mass end of the Li dip, around 1.0 $M_{\odot}$). Intermediate-mass polluted stars will show a decrease in [Fe/H] with increasing mass, up to M_{dip}, followed by a sharp increase at M_{blue}.

We want to stress that, while we are using the lithium data as a proxy to estimate the depth of the surface mixing layer of main-sequence solar-type stars, and while we anticipate that the surface abundances of lithium and iron will follow similar patterns, the reason for the abundance variations differ. The lithium abundances vary because lithium is destroyed when it is mixed below the surface of the star. Stars in the mass range we consider neither destroy nor create iron. Rather, we assume that some iron is added to the surface of the star after it forms; it is then diluted by the mixing process down to the same depth to which lithium is mixed. In other words, the variations in lithium are produced by the destruction of lithium inside the star while the variations in iron are produced by the addition of iron from outside the star.

4. OBSERVATIONAL CONSTRAINTS ON POLLUTION

To look for mass-dependent variations in [Fe/H], we must be able to estimate the masses of stars, and we must have reliable measurements of the metallicity. To find the mass of a star, we need to know its luminosity or, alternately, its absolute V magnitude, M_v, its colors (we use $B-V$), and its composition, [Fe/H]. The *Hipparcos* catalog gives parallaxes accurate to roughly 1 mas for a selection of stars in the solar neighborhood, allowing us to find absolute magnitudes when we are given V. We use SIMBAD values for B and V. We take metallicities from the Cayrel de Strobel et al. (1997) catalog. This lists spectroscopically determined values for [Fe/H] taken from the literature.

We take all the HD stars in the Cayrel de Strobel et al. catalog for which there are *Hipparcos* parallaxes larger than 10 mas (corresponding to distances less than 100 pc). We also require that the error in the parallax be less than 10%. Since we are interested in main-sequence stars that have masses less than about 2 $M_{\odot}$, we eliminate all stars with $M_v < 1.0$.

We then fit the remaining stars to stellar tracks taken from a grid of models having $-0.5 \leq$ [Fe/H] ≤ 0.5 in steps of 0.05 dex and masses in the range $0.60 \leq M \leq 1.75 \, M_{\odot}$ in steps of 0.05 $M_{\odot}$. These models were calculated using Chaboyer's version of the Yale stellar evolution code (Guenther et al. 1992). These models incorporate the following input physics: high-temperature opacities from Iglesias & Rogers (1996); low-temperature opacities from Alexander & Ferguson (1994); nuclear reaction rates from Bahcall & Pinsonneault (1995) and Bahcall (1989); helium diffusion coefficients from Michaud & Proffitt (1993); and an equa-

tion of state that includes the Debye-Hückel correction (Guenther et al. 1992). The stellar models employ a solar calibrated mixing length. The models were evolved from the completely convection pre–main-sequence phase to the giant branch in ~ 800 time steps. In each time step, the stellar evolution equations were solved with a numerical accuracy exceeding 0.01%. The models did not include any overshooting beyond the formal edge of the convection zones.

All models employed a scaled solar composition (Grevesse & Noels 1993). Our calibrated solar model had an initial solar helium abundance of $Y = 0.258$ and heavy-element mass fraction of $Z = 0.0185$. Assuming a primordial helium abundance of $Y = 0.234$ (Olive, Steigman, & Skillman 1997), our calibrated solar model implies $\Delta Y/\Delta Z = 1.3$. This value of $\Delta Y/\Delta Z$ was used to calculate the helium abundance for the [Fe/H] values that were less than solar. For the above solar metallicities, a value of $\Delta Y/\Delta Z = 2.0$ was used, as this provides the best fit to the super–metal-rich cluster NGC 6791 (Chaboyer, Green, & Liebert 1999). Values of Y and the conversion between [Fe/H] and Z were determined using the standard formulae:

$$Y = Y_{\odot} + (\Delta Y/\Delta Z)(Z - Z_{\odot}) \qquad (7)$$

and

$$[\text{Fe/H}] = \log (Z/Z_{\odot}) - \log (X/X_{\odot}) . \qquad (8)$$

The stellar evolution tracks were transformed from the theoretical ($\log L$, $\log T_{eff}$) plane to observed colors and magnitudes using color transformations and bolometric corrections from Yi (1998, private communication) that are based on the Kurucz (1993) model atmospheres. Chaboyer et al. (1999) provide further details on the color transformation.

In the course of our analysis, a problem with our stellar models became apparent. Stars with $B-V > 1$ were systematically found to be older than 20 Gyr. We believe that this is because of a failure of our atmospheric models at this low effective temperature. As a check, we made a detailed comparison between the transformed models and the absolute magnitude $B-V$ diagram of de Bruijne, Hoogerwerf, & de Zeeuw (2000). We found good agreement between the models and the data for $B-V < 1.0$. For $B-V > 1.0$, the models are redder than the observations, which will lead to physically unrealistic old ages for the lower mass stars in our sample.

We call a star evolved if it has a convection zone mass more than 10 times larger than the mass of the surface mixing layer at an age of 10^8 yr, while the absolute V magnitude has not decreased by more than ≈ 0.5. We refer to such stars as "Hertzsprung gap" stars. This occurs roughly when the star leaves the main sequence. It is a useful definition because it allows us another check on the pollution scenario; if pollution is occurring, the class of stars with convection zone masses 10 times larger than their initial main-sequence convection zone masses should show substantially lower [Fe/H] values than their parent populations.

If the absolute V magnitude has decreased by more than ≈ 0.5, the star is considered to be a giant. Because their surface gravities are so much lower than main-sequence stars of the same mass, we hesitate to compare the metallicity trends of giants and dwarfs.

Of the 640 stars in our sample, 466 were unevolved and had masses in the range $0.8 \leq M \leq 1.8$. Fifteen stars had convection zones 3–10 times larger than their main-sequence value (at 10^8 yr); we treated these as unevolved. Nineteen stars had convection zones more than 10 times as massive as the main-sequence values; these are our Hertzsprung gap stars. The remainder of the stars were either giants or were not well fit by our models; most of the latter were red, low-mass stars.

In Figure 3 we plot [Fe/H] against stellar age, while Figure 4 shows [Fe/H] plotted against stellar mass. The metallicity decreases with increasing age and increases with increasing mass. We also note that the Hertzsprung gap stars tend to have lower metallicity than unevolved stars of the same age and mass. Figure 5 shows the histogram of [Fe/H] for our sample. It is well fit by a Gaussian distribution with mean $\langle[\text{Fe/H}]\rangle = -0.095$. The dotted line in the figure shows the histogram for the Hertzsprung gap stars. The mean $\langle[\text{Fe/H}]\rangle = -0.2$ for the latter. Once again it appears that the Hertzsprung gap stars have lower metallicity than main-sequence stars. The Kolmogorov-Smirnov test indicates that the probability that the two samples are drawn from the same distribution is 0.02.

The trend with stellar age is expected on the basis of chemical evolution; younger stars are constructed using gas that has been contaminated by material processed in the interiors of massive stars. The more recent the stellar birth, the higher the fraction of processed material. The trend is seen even more clearly when we bin the data by age, as seen in Figure 6. The slope of a least-squares fit to the [Fe/H] versus log (age) curve is -0.21 dex per log Gyr. Edvardsson et al. (1993), studying a proper subset of our sample, find a slope of -0.39 ± 0.21, while Meusinger et al. (1991) find a slope with a slightly larger magnitude.

FIG. 4.—Stellar metallicity as a function of stellar mass, where the mass is obtained by fitting to our stellar models. As in Fig. 3, filled squares represent unevolved stars, while open triangles represent evolved stars.

The trend of increased metallicity with increased stellar mass might arise from the age-metallicity trend combined with the short lifetimes of massive stars. Since the stars we consider are either unevolved or only slightly evolved, they must have ages less than or roughly equal to their main-sequence lifetimes. Massive stars have short lifetimes and,
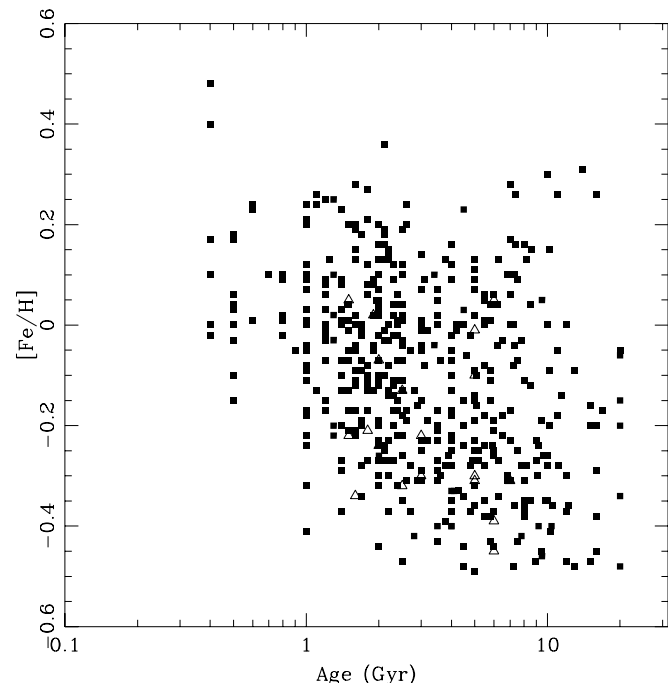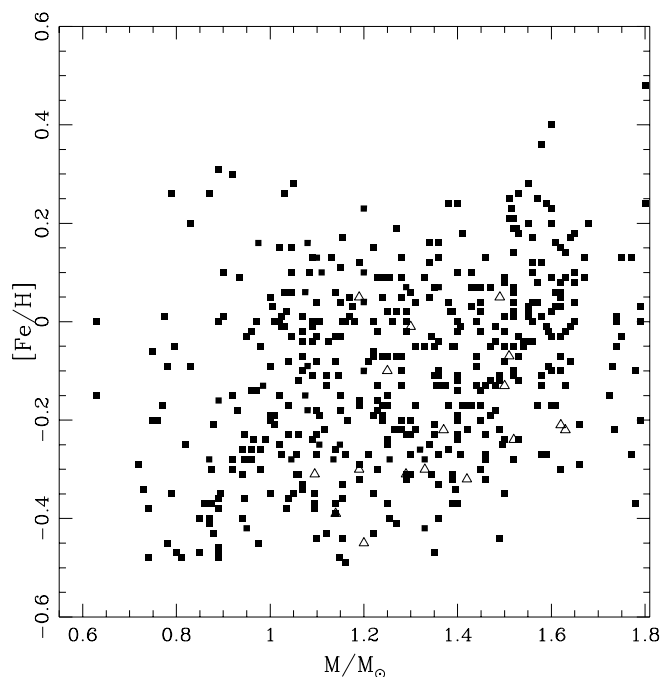

FIG. 3.—Stellar metallicity as a function of the logarithm of the stellar age, where the latter is obtained by fitting to our stellar models. Filled squares represent unevolved stars while open triangles represent evolved stars (dwarf stars with surface convection zones 10 or more times larger than M_{mix}).
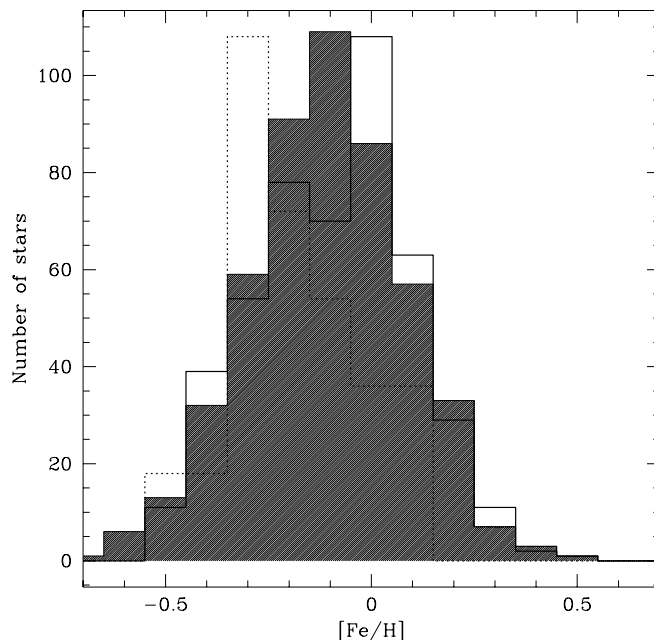

FIG. 5.—Histogram of stellar metallicity for 466 main-sequence stars (thick solid line) and for 19 Hertzsprung gap stars (dotted line). The latter histogram has been multiplied by 18 to make comparison between the two easier. The best-fit Gaussian distribution (not shown) for the main-sequence stars has mean $\langle[\text{Fe/H}]\rangle = -0.095$ and variance $\sigma = 0.18$; for the Hertzsprung gap stars, the values are -0.20 and 0.20. The shaded histogram is from a Monte Carlo model of 466 stars. These stars are polluted with a mean mass of 0.4 $M_\oplus$ of iron. See the text for a more detailed description of the model.
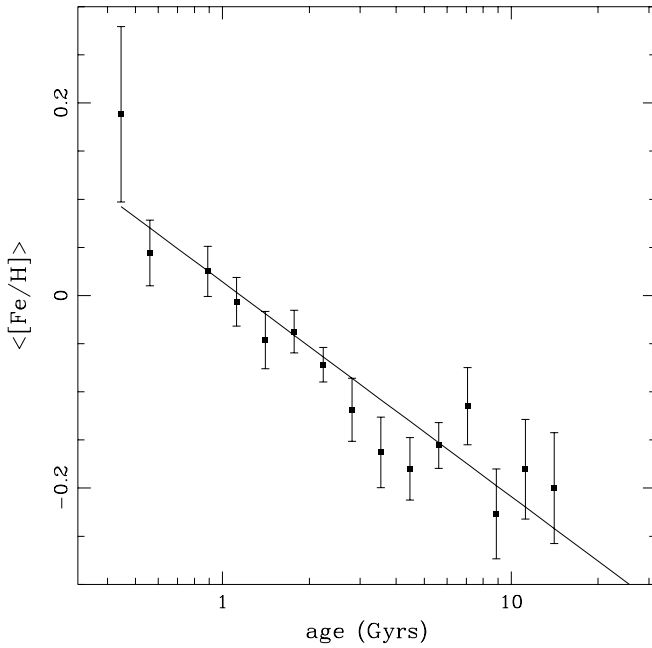
FIG. 6.—Average stellar metallicity in age bins of width $\Delta \log (\text{age}) = 0.1$. There are roughly 30 stars per bin. The straight line is a least-squares fit having slope -0.21 dex/log (Gyr).

hence, low ages (see Fig. 7). They will therefore be more metal rich, on average, than less massive stars.

The next section will show that while part of the variation of metallicity with stellar mass is caused by the age-metallicity relation, it is not the whole story.

5. MONTE CARLO MODELS OF POLLUTION

The data suggest a possible trend of surface [Fe/H] with stellar mass. In order to evaluate the significance of this
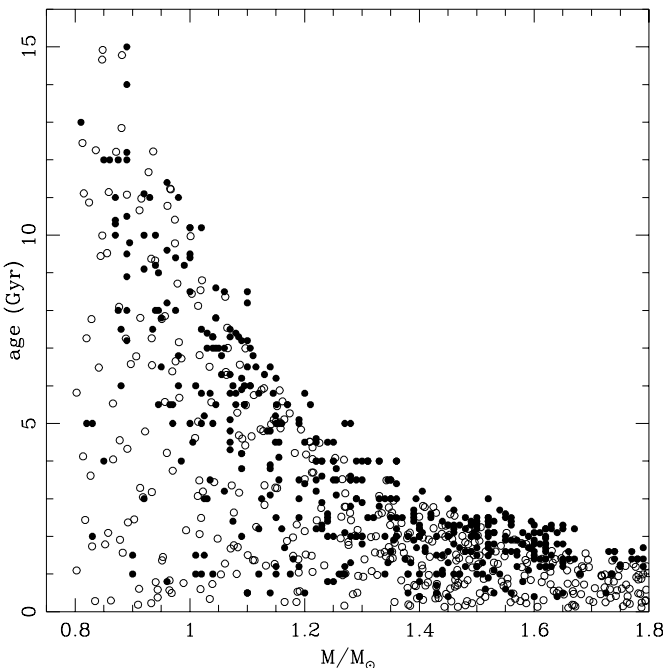

FIG. 7.—Stellar age plotted against stellar mass. Note that, on average, the more massive stars are younger. Filled circles are actual stars, open circles are Monte Carlo results. It is this relation that produces the apparent mass-metallicity trend seen in the unpolluted Monte Carlo model represented by the dotted line in Fig. 8.

trend, we have undertaken Monte Carlo experiments to calculate the predicted metallicity of a population of polluted stars.

We start by producing a population of unpolluted stars having the same characteristics as the Cayrel de Strobel–derived sample described above. This involves generating a sample of stars with mass roughly uniformly distributed between 0.8 and 1.8 $M_\odot$, with metallicities Gaussian distributed about an age-dependent mean. From our sample of stars, and using a simple two-parameter fit, we find that the mean [Fe/H] is given by

$$\langle [\text{Fe/H}] \rangle = \alpha + \beta \times \log (\text{age}) , \qquad (9)$$

where $\alpha = 0.03$ and $\beta = -0.21 \pm 0.02$. The width of the [Fe/H] distribution is slightly age-dependent, but we assume an age-independent width $\sigma = 0.18$.

We constrain the stellar age to be less than the calculated lifetime of the star. As noted above, we define the lifetime of a star to be the age at which the mass of the surface convection zone exceeds 10 times the mass of the mixed surface layer at an age of 100 Myr. Our stellar models have lifetimes (as defined above) that vary as the 3.65 power of the stellar mass,

$$L\left(M_*, \left[\frac{\text{Fe}}{\text{H}}\right]\right) = M_1\left(\left[\frac{\text{Fe}}{\text{H}}\right]\right) \times \left(\frac{M_*}{M_\odot}\right)^{-3.65} , \qquad (10)$$

where

$$M_1([\text{Fe/H}]) = 11.5 + 4.5[\text{Fe/H}] \text{ Gyr} \qquad (11)$$

is the lifetime of a one solar mass star of metallicity [Fe/H].

Using this prescription, we generate 466 stars, yielding the mass-age relationship depicted by the open circles in Figure 7; the agreement with the observed age-mass relationship is very good.

5.1. The Unpolluted [Fe/H]-Mass Correlation

We can use this Monte Carlo model to see if the [Fe/H]-mass correlation seen in our sample could be caused simply by the known age-mass and age-[Fe/H] correlation. To repeat, the idea is as follows: massive stars are necessarily young. Young stars are metal rich, since they form out of gas that has been processed through many generations of high-mass (supernova-producing) stars. Thus, more massive stars should have higher metallicity than less massive stars.

This argument is partially borne out by the Monte Carlo model. We adjusted the slope of the [Fe/H] versus logarithm of stellar age relation to obtain agreement with that seen in our sample [-0.21 dex per log (Gyr)], then examined the metallicity as a function of stellar mass. The stellar metallicities do show a dependence on stellar mass. However, the slope of the [Fe/H] versus mass relation for the observed stars is 0.26 ± 0.03 dex per solar mass while that of the unpolluted Monte Carlo model is 0.18 ± 0.03, different by 3 standard deviations.

A second indication that there is a real mass dependence in the data comes from allowing for a third parameter in a least-squares fit. Heretofore, we have used a two-parameter fit, an age-metallicity slope, and an intercept. If we allow for a linear variation of [Fe/H] with mass, the slope of the fit is a third parameter. A fit of the form

$$\left[\frac{\text{Fe}}{\text{H}}\right] = \alpha + \beta \log (\text{age}) + \gamma \left(\frac{M}{M_\odot}\right) \qquad (12)$$

does give a significantly improved chi squared.

To see if this three-parameter fit can really distinguish between a pure age dependence and a mixed age and mass dependence, we modified our Monte Carlo model to allow for a linear dependence of average metallicity on stellar mass. We then ran the resulting stars through our least-squares routine. If we set the amount of added iron to zero but force an age dependence, the least-squares fit finds the correct age-metallicity slope. It also correctly finds that there is no mass dependence despite the apparent dependence in a metallicity versus mass plot. If we introduce a mass dependence into the model, the least-squares fit correctly finds both the age and mass dependences. Finally, we produced samples of stars with a mass dependence but no age dependence. A plot of metallicity versus age clearly shows a trend; this is expected since we force the more massive stars, which are younger, to have higher metallicities. Despite this apparent age-metallicity trend, the linear least-squares fit finds the correct mass-metallicity slope and a zero slope for the age-metallicity relation.

Edvardsson et al. (1993) showed that the metallicity of stars in the Galaxy depends not only on age, but also on the radial distance from the Galactic center. We examined the effect of allowing for a fourth parameter, R_M, the average stellar distance from the Galactic center, for a subset of our sample taken from Gustafsson et al. (1999). Allowing for this dependence, either by itself or in combination with an age or mass dependence, does not give a better fit to the data in our sample.

These results suggest that the real data exhibits a mass trend independent of stellar age. More compelling evidence is obtained by comparisons with more sophisticated models. The inadequacy of a simple age-dependent metallicity is most clearly seen by examining the binned metallicity versus mass distribution (Figure 8). Another indication is the poor reduced χ^2 (χ^2/dof) of the fit; the best unpolluted model, shown as the dotted line in the figure, gives $\chi^2/\text{dof} = 3.2$ for the binned distribution.

Note that the error bars in the figure do not account for any systematic errors so that the actual error bars should be somewhat larger, reducing the χ^2 significance of the deviations from an unpolluted model. We do not know how to estimate the systematic errors in our rather heterogeneous sample; we simply warn the reader that they exist and urge observers to produce better controlled samples. We proceed to examine more realistic polluted models, which give substantially better fits to the data.

5.2. Realistic Polluted Models

As noted above, pollution introduces a third free parameter, the amount of iron added to the star. In the last subsection, we assumed that [Fe/H] increases linearly with stellar mass. This is not what we expect from pollution since the mass of the surface mixing layer is not linear or even monotonic with stellar mass. In this subsection, we assume a Gaussian distribution of accreted mass with a variance equal to half the mean. Stars allotted a negative amount of accreted mass by this process are assumed to have no added material. We assume the accreted mass is mixed over a surface layer of mass M_{mix}, as described in § 3.1. Our model for the mass of the surface mixing layer has many parameters, but we hold all of them except M_{mb} fixed at the values given in that section. The single adjustable parameter is then the mean mass of accreted iron (assumed to be independent of stellar mass). We adjusted this mean to obtain a
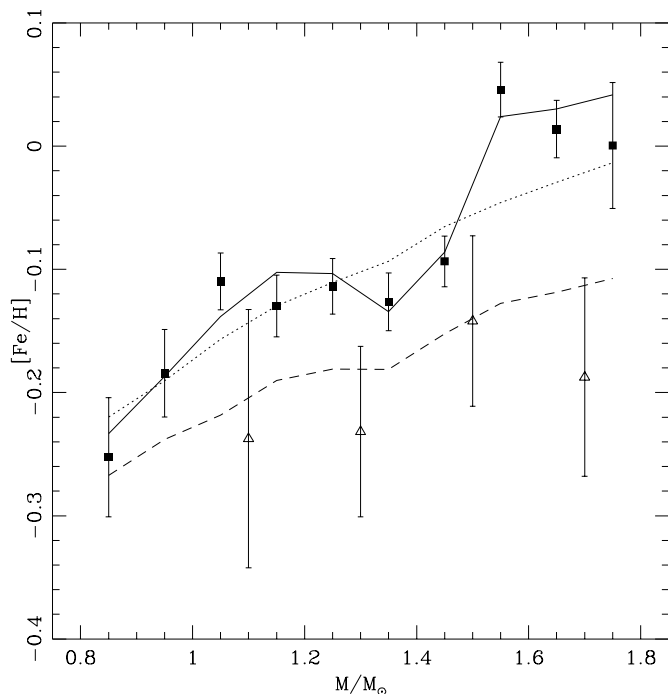

FIG. 8.—Average stellar metallicity in mass bins of width 0.1 $M_\odot$ (filled squares represent unevolved stars). There are roughly 45 such stars per bin. Error bars are the standard deviation of the mean of the values in each bin. Open triangles represent the evolved stars (dwarf stars with surface convection zones 10 or more times larger than M_{mix}). There are only 3–6 stars per bin, with a bin width of 0.20 $M_\odot$ for these objects. The evolved stars appear to have lower metallicity than unevolved stars of the same mass. The dotted line is the unpolluted Monte Carlo model giving the smallest reduced $\chi^2 = 3.2$. The solid line is the polluted Monte Carlo model having $M_{\text{mb}} = 3 \times 10^{-3} M_\odot$. This model has an accreted iron mass of 0.4 $M_\oplus$ and an intrinsic age-metallicity slope of -0.14 dex per log Gyr (giving a slope of -0.21 in a plot of [Fe/H] vs. log age); the fit has a reduced χ^2 of unity. The model with $M_{\text{mb}} = 5 \times 10^{-3} M_\odot$ gives a similar fit but with a smaller dip at $M = 1.4 M_\odot$; it also requires more accreted iron, about 0.6 $M_\oplus$. The dashed line is the polluted model after the mass of the surface mixing region has increased by a factor of 10 from its main-sequence value and should be compared to the evolved star data represented by the open triangles. This fit also has a reduced χ^2 of order unity.

minimal reduced χ^2 in the binned data, both metallicity-mass and metallicity-age. The resulting fit to the metallicity-mass data is shown as the solid line in Figure 8. We were able to find fits with reduced χ^2 equal to one.

The intrinsic slope of the age-metallicity relation in the polluted models (-0.14 dex per log Gyr) has a smaller magnitude than that of unpolluted models (-0.21 dex per log Gyr). Note that we required that the apparent slope match the observed value -0.21 for both models. This result has important consequences for models of the star formation history of the Galaxy.

We explored models with larger surface mixing zones M_{mb} in stars above 1.5 $M_\odot$. We could find similar fits, but naturally the required mass of added material is larger, up to 0.6 $M_\oplus$.

The detailed variation of [Fe/H] with stellar mass, including the steep increase starting at 0.8 $M_\odot$, the dip around 1.4 $M_\odot$, and the steep increase to 1.5 $M_\odot$ seen in the binned data is reasonably similar to that seen in the model. We feel that the low reduced χ^2 and the detailed variations of metallicity with mass offer strong support both for (1) a mass-dependent mixing, as suggested by the Li dip; and (2)
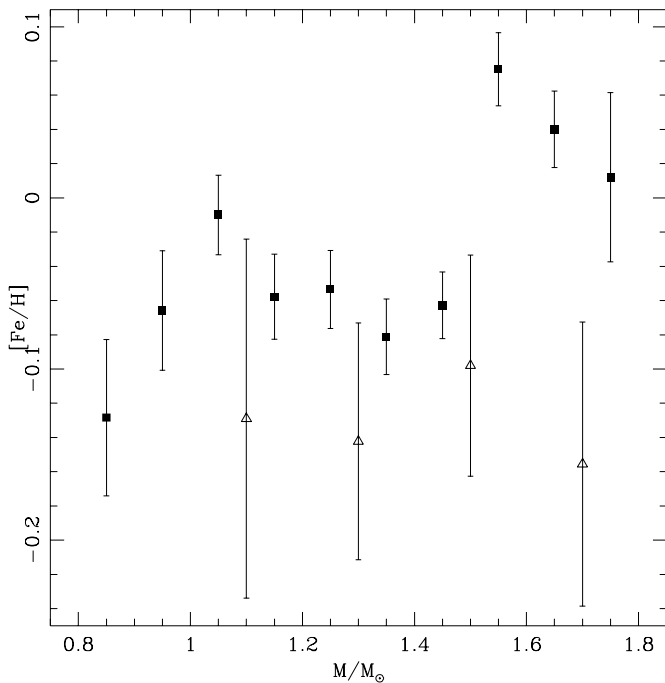
FIG. 9.—Average metallicity, adjusted for age using the slope found in our best-fit polluted model (a slope of -0.14 dex per log Gyr). This figure should be compared to plots of lithium abundance showing the lithium dip.

for accretion of ~ 0.4–0.6 $M_\oplus$ of iron in most stars in the solar neighborhood.

5.3. *Hertzsprung Gap Stars*

The metallicity-mass trend, combined with the jump in average [Fe/H] around 1.5 $M_\odot$ strongly suggests that stars in our sample have accreted iron-rich material. However, the properties of our sample are not well constrained since the selection criteria of the various samples collated by Cayrel de Strobel are difficult to ascertain. Perhaps the apparent variations in average metallicity are caused by some unknown selection effect. For example, one of the subsamples is that of Favata, Micela, & Sciortino (1997). A plot of [Fe/H] versus mass for this sample shows an increase toward large masses, starting at about 1.15 $M_\odot$. However, this sample was selected to have $B-V > 0.5$; this eliminates low-metallicity, high-mass stars, which are bluer than this limit. This is the origin of the increase in [Fe/H] at 1.15 $M_\odot$ in this subsample.

We do not see an increase in [Fe/H] at 1.15 $M_\odot$ in the large sample. However, perhaps the sharp jump we see at 1.5 $M_\odot$ is because of a similar selection effect. The best way to eliminate this possibility would be to perform an unbiased survey of a large number of stars in the solar neighborhood. We encourage observers to undertake such a survey.

However, we do have available to us a small control sample that indicates that the jump we see in [Fe/H] is not a selection effect. Stars that are slightly evolved, in the sense that their convection zones are 10 or more times larger than those on the main sequence, but which are not yet giants (having M_v within 0.5 of the main-sequence value), provide a check on our interpretation. These stars sit in the Hertzsprung gap. Unlike giants, their surface gravities and fluxes are very similar to stars on the main sequence, so their

metallicities can be compared directly with those of main-sequence stars.

If pollution is responsible for the [Fe/H] variations over and above those caused by age effects, then Hertzsprung gap stars should have lower average metallicities.

The open triangles in Figure 4 represent the metallicities of stars in the gap. It is apparent that these stars have, on average, slightly lower metallicity than unevolved stars of similar mass. This is confirmed by an examination of the binned data (Fig. 8). This provides support for the notion that the variations in metallicity with mass seen in the unevolved stars are caused by pollution.

The dashed line in Figure 8 shows the predicted [Fe/H] for the same model as the solid line but where the mass of the accreted material has been reduced by a factor of 10. This is equivalent to increasing the mass of the surface mixing layer by the same factor. The predicted metallicity for this population is lower than that predicted for the polluted sample and shows only a hint of a "lithium" dip, although given the large error bars one could easily be present. It gives an acceptable fit to the rather sparse observational data (reduced χ^2 less than one).

We looked at the variation of metallicity with average distance R_M from the Galactic center in § 5.1 to see if the birthplace of the stars might have influenced their metallicity, thus producing the variations we see. As a second check that these variations in metallicity with mass are not an artifact of the kinematics of the sample, we examined the stellar metallicity as a function of transverse velocity. We find a clear trend, in that less massive stars have higher transverse velocity. This is expected since these low-mass stars are older and have suffered more random velocity kicks than younger (more massive) stars. However, there is no sign of any peculiar kinematics.

In plotting both the data and the fit in the metallicity-mass plots, we have not adjusted [Fe/H] according to the star's age. In Figure 9 we replot the data adjusting for the age-metallicity trend using the measured slope of the age-metallicity relation in Figure 6. This involves increasing the [Fe/H] for old stars. This figure should be compared with plots of lithium abundance in clusters; we see evidence of a "lithium" dip in the iron data similar to that seen in lithium data. The dip is less distinct in the iron data, a fact we attribute to the range of metallicities in our sample (the metallicities in cluster stars show much smaller dispersions). The variation in metallicity produces a variation in the mass of the dip, so combining stars with different metallicity will tend to smear out the dip. This smearing is clearly seen in our Monte Carlo models (the solid line in Fig. 8).

We have also examined the metallicities of giants in our sample. They show a slight increase in [Fe/H] with mass, but this increase is consistent with the age-[Fe/H] correlation. The average [Fe/H] is actually slightly *larger* than either the unevolved stars or the Hertzsprung gap stars, although consistent within the rather large errors. However, given the very different environment for line formation in these stars, we do not feel it is appropriate to make a direct comparison between the two populations.

6. DISCUSSION

We made use of three free parameters in fitting the metallicity-age and metallicity-mass data: one for the slope of the metallicity-age relation, one (the mean of the added mass) for the correlation in the metallicity-mass relation,

and an overall normalization. We want to stress that, in fitting the Hertzsprung gap star data (both age and metallicity), we did not adjust any free parameters.

We also had a number of parameters in the model that were fixed by other observations; most were used to describe the location and depth of the lithium dip. The most critical for our purposes is the mass $M_{mb} = 3$–5×10^{-3} $M_{\odot}$ of the surface mixing layer in stars blueward of the dip. Varying this mass directly affects our estimates of the amount of iron accreted onto the star. Varying M_{mb} over the indicated range changes our estimate from 0.4 to 0.6 $M_{\oplus}$ of accreted iron. However, the need to accrete *some* material is not uncertain; reducing M_{mb} will reduce the inferred mass of accreted material, but models with no pollution will still fail to fit the data.

The linear model for the mass of the surface mixing layer we employ is unlikely to be correct in detail; the V-shaped bottom is particularly questionable. Future work should employ a more realistic model for M_{mix}, but for this first foray we did not feel that more realistic models were necessary, nor would they be well founded physically.

The jump in [Fe/H] seen in Figure 8 at 1.5 $M_{\odot}$ coincides with the disappearance of the surface convection zone. It also coincides with a jump in stellar rotational velocity (see, e.g., Balachandran 1995). Could the jump be an observational artifact caused by the broader iron lines in the rapidly rotating stars? To check this possibility, we collected rotation data from the literature (Mathioudakis et al. 1995; de Medeiros & Mayor 1999). Our sample does display a jump in $\langle V \sin i \rangle$ around 1.5 $M_{\odot}$; for main-sequence stars with $M_* < 1.4$ $M_{\odot}$, we find $\langle V \sin i \rangle = 6.2$ km s^{-1}, while for stars with $M_* > 1.5$ $M_{\odot}$ we find $\langle V \sin i \rangle = 20.5$ km s^{-1}. However, a plot of [Fe/H] versus $V \sin i$ for stars more massive than 1.5 $M_{\odot}$ shows no trend; stars with small $V \sin i$ have the same (high) metallicity as stars with large $V \sin i$. This suggests that the metallicity jump is not because of the change in stellar rotational velocity affecting the estimate of the stellar metallicity.

Similarly, an examination of the kinematic properties of the sample does not reveal any feature in the distribution of average distance from the Galactic center or in the distribution of stellar velocities that would explain the metallicity pattern we see.

The Hertzsprung gap stars afford a check on our interpretation of the metallicity pattern as a pollution effect. From Figure 8, the massive (>1.5 $M_{\odot}$) evolved stars are nearly 0.2 dex less metal rich than unevolved stars of the same mass, on average. We have argued above that this is because of the presence of a massive convection zone in the evolved stars, while the main-sequence stars lack convection zones. The elevated metallicity seen in polluted main-sequence stars should be reduced when the convection zone appears. This appears to be the case in our sample.

If the evolved stars do have convection zones, they should have magnetic fields, and thus they should lose angular momentum in stellar winds and spin down. In fact, the average $\langle V \sin i \rangle = 3.4$ km s^{-1} for these five stars, with a maximum around 7 km s^{-1}. This bolsters our confidence in stellar modeling; the evolved stars do appear to be spun down, which is consistent with the notion that they have massive convection zones. But is the apparently low metallicity caused by the deepening convection zone diluting accreted iron or by the different (rotationally induced) widths of the line profiles? We checked the latter possibility by

selecting unevolved stars with $\langle V \sin i \rangle$ less than 10 km s^{-1} (we have only five of these as well). We find an average metallicity of 0.15, indicating that the difference in metallicity between main-sequence and Hertzsprung gap stars is not an observational artifact caused by the difference in rotational velocities of the two populations.

As just noted, the surface metallicity of the more massive unevolved stars in our sample appears to be about 0.2 dex higher than the bulk metallicity. To be self-consistent, we should, in principle, estimate the masses and ages of these stars using polluted stellar models. We have not done so since, when we undertook this work, we did not have such models available to us. We now have a working code for making such models in hand and will employ it in future work.

If the trends we see are caused by pollution, one might surmise that stars with larger [Fe/H] will form with more massive planetesimal disks. This might result in larger amounts of iron-rich material falling on stars with larger intrinsic metallicities. This could be modeled by assuming a correlation between [Fe/H] and the amount of added material; once again, we leave such experiments for later work.

6.1. Gas Migration and Ingestion of Gas Giant Planets

The gas giant planets in our solar system appear to have rock/ice cores with masses of order 10 $M_{\oplus}$, with the possible exception of Jupiter (Guillot 1999a), which could lack such a core. These cores are believed to form at $\gtrsim 5$ AU from the Sun since the surface density of solid matter in the protoplanetary disk is believed to jump up beyond that distance because of the presence of ice. The discovery of Jupiter-mass planets in small (less than 0.05 AU) orbits around solar-type stars motivated a number of groups to suggest that gas giant planets migrate. If this migration is overly efficient, Jupiter-mass objects may be accreted onto the star. In the leading theory of planetary migration, that of tidal interactions between massive planets and the gas disk out of which they formed, the migration time is given by the viscous evolution time of the disk, prompting many authors to predict such accretion (Lin 1997; Laughlin & Adams 1997). Others have suggested accretion of iron-rich material originally between the planet and the star (Gonzalez 1997).

There are two distinct scenarios. In the first, iron-rich material is pushed onto the star by the gaseous disk. This material necessarily falls on the star before the gas disk disappears, when the star is between one and 10 million years of age. In the second, the enriched material arrives via some other mechanism, after the gas disk disappears. The primary difference between the two, from the point of view of pollution, is the depth of the stellar convection zone; stars younger than 10 million years and less massive than ~ 1.3–1.4 $M_{\odot}$ have very massive convection zones and consequently are difficult to pollute.

Laughlin & Adams (1997) showed that stars less massive than ~ 1.3–1.4 $M_{\odot}$ will not exhibit any detectable change in [Fe/H] even if they accrete Jupiter-mass planets up to 10 Myr after the star forms. We have reproduced their calculation and find the same result.

Laughlin & Adams do find that more massive stars could be slightly polluted by this early accretion. However, they do not consider that the gas causing the migration, which must necessarily be more massive than the planet, dilutes

the effect of the planet. Here we attempt to include the *minimum* possible dilution effect to see the *maximum* possible pollution by the planet and gas combined.

Suppose that the star and gas disk initially have mass fraction z_0 in metals. Suppose that a planet with mass m_p and metallicity z_p forms in the disk and depletes metals from a mass Nm_p of gas, leaving it with metal content z_d. The conservation of the total amount of metals in the gas plus that in the planet then implies $(N + 1)z_0 = z_p + Nz_d$. Assume that a fraction $1 - f$ of the depleted gas is either removed by a wind, or falls into the star while the convection zone is still massive. (In the latter case, accreting metal-poor material will hardly reduce the surface metallicity since the mass of depleted gas is small compared to that of the convection zone.) Also ignore any nondepleted gas in the disk that lies well outside the orbit of the planet, as this gas will only decrease the metallicity of the mixing region below that given in the estimate below. We will focus solely on the effect of the planet and the fraction f of depleted gas that falls onto the star. Assume that the gas falls onto the star at a similar time as the planet, since if it falls onto the star much later the convection zone will have thinned; this would decrease the apparent metallicity of the stellar photosphere.

For a mixing region of size M_{mix} and initial metallicity z_0, the metal content after pollution is

$$z_{after} = \frac{M_{mix}z_0 + m_p z_p + fNm_p z_d}{M_{mix} + m_p + fNm_p}, \quad (13)$$

or

$$\frac{z_{after} - z_0}{z_0} = (1 - f)\frac{(z_p - z_0)/z_0}{M_{mix}/m_p + 1 + fN}. \quad (14)$$

As one expects, if $f = 1$ and all depleted gas falls onto the star along with the planet there is no increase in metallicity. For fixed $f < 1$, the amount of pollution decreases with increasing N. A minimum value of N, which gives maximum pollution, is found by assuming that all the metal originally in the depleted gas enters the planet, in which case $z_d = 0$; this minimum N is given by $N = z_p/z_0 - 1$. In this case, the maximum pollution possible is

$$\left(\frac{z_{after} - z_0}{z_0}\right)_{max} = (1 - f)\frac{(z_p - z_0)/z_0}{M_{mix}/m_p + 1 + f(z_p/z_0 - 1)}. \quad (15)$$

We compare accretion of a planet with and without gas in Figure 10. For ease of comparison, we use the "standard model" of Laughlin & Adams, which has a disk age of 10 Myr and a shape parameter for the time of accretion $n = 2$. We choose the unpolluted stars as in our Figure 8 in order to compare with the data, but we use the mixing zone mass from Laughlin & Adams. (Note that this assumes the low-mass stars are unpolluted, an assumption that our results call into question.) The filled squares show the data; the dotted line, the unpolluted model stars; the solid line, the pollution by a planet only ($f = 0$ as in Laughlin & Adams; and the dashed line shows the *maximum* pollution possible when the gas is included. We have used $f = \frac{1}{2}$ for the fraction of depleted gas which falls onto the star after the disk has thinned.
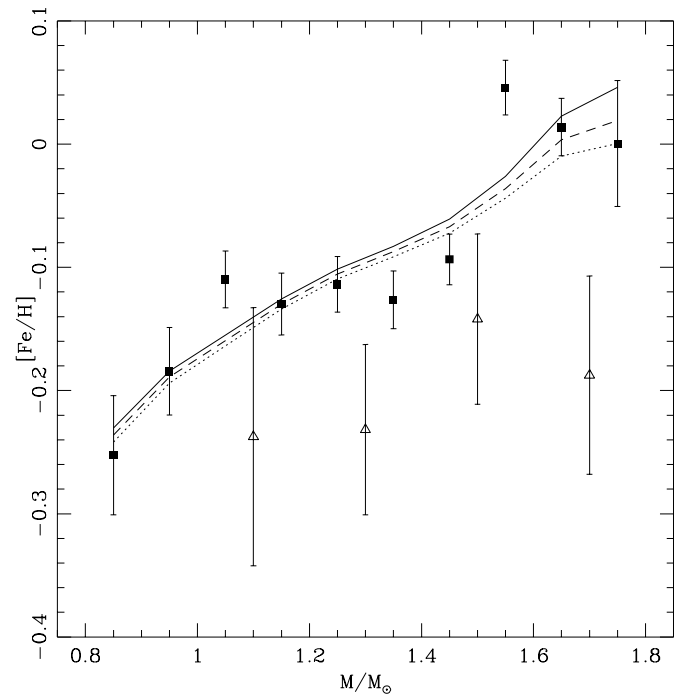

FIG. 10.—Metallicity vs. mass, showing the same data as in Fig. 8 and the "standard model" for gas-disk driven planet accretion of Laughlin & Adams (1997, their Fig. 2). The solid line is the Laughlin & Adams model, which assumes that planets are pushed into the star, but which does not account for the accretion of the accompanying metal depleted gas (see the text). The dotted line is the best-fit unpolluted model while the dashed line is a polluted model similar to that of Laughlin & Adams but assuming that 50% of the gas that supplied the excess metals to the planet is ingested along with the planet.

We find that although stars with masses above 1.4 $M_\odot$ are preferentially polluted by planets, the effect is only of order ~ 0.02 dex when $f = 0$. This is similar to the result of Laughlin & Adams for their "standard model."

A more realistic model has $f > 0$, leading to a smaller enhancement in [Fe/H]. Observationally, disk winds appear to remove 3%–30% of the mass in the disk in classical T Tauri systems (Calvet 1997; Richer et al. 2000), in agreement with theoretical estimates (Konigl & Pudritz 2000; Shu et al. 2000). This would leave the bulk of the material in the inner disk to be accreted onto the star. In fact, there is strong observational evidence for accretion onto the surfaces of young stars (Muzerolle, Calvet, & Hartmann 1998; Gullbring et al. 2000). If the planet plunged into the star at the same time, $f = 0.7$–0.97.

Jupiter-mass objects may well be accreted onto stars during the evolution of the circumstellar gas disk. However, the fact that the net change in metallicity of the star will be small, combined with the poor fit of the model to the evolved star data, suggests that accretion must also occur after the accretion disk vanishes, providing the bulk of the apparent pollution.

6.2. Ingestion of Gas Giants by Other Means

Lin (1997) speculates that Jupiter-mass planets might survive the gas disk only to fall onto the star later. If this occurs, and if these objects have heavy element abundances similar to gas giants in our solar system, then the star will gain ~ 1.8 $M_\oplus$ of iron for each Jupiter-mass of accreted material. We can find acceptable fits to the data in Figure 8

if roughly 30% of stars in the solar neighborhood have each accreted a single Jupiter-mass body *after* their convective envelopes thinned. These models naturally predict that the average metallicity of such stars will decrease by the observed amount when their convection zones deepen at the end of their main-sequence lifetime.

However, we have more information available to us than just the mean metallicity as a function of stellar mass. In particular, we know that the distribution of [Fe/H] is well fit by a Gaussian distribution, as illustrated in Figure 5. This fact allows us to rule out pollution dominated by late ingestion of Jupiter-mass planets having iron contents similar to that of the giant planets in our solar system. The idea is to use the sensitivity of the high-mass stars to pollution. Adding $\sim 1.8\ M_\oplus$ of iron in discrete lumps to 30% of these stars (to give the observed mean [Fe/H]) will produce a population with metallicities about three times that of the unpolluted population in these high-mass stars. Using the Monte Carlo model that reproduces the variation of mean metallicity mentioned in the previous paragraph, we obtain the two-peaked histogram shown in Figure 11. This can be compared with the observed distribution for those stars above $1.4\ M_\odot$ shown on the same figure. If these stars are in fact polluted, the pollution is distributed smoothly over most of the stars rather than being concentrated in a fraction of order 30%. We conclude that the metallicity trend we find is not produced simply by the late ingestion of Jupiter-mass objects.

More complicated models, involving the ingestion of Jupiter-mass planets at early times, could produce the observed distribution by careful tuning of the accretion
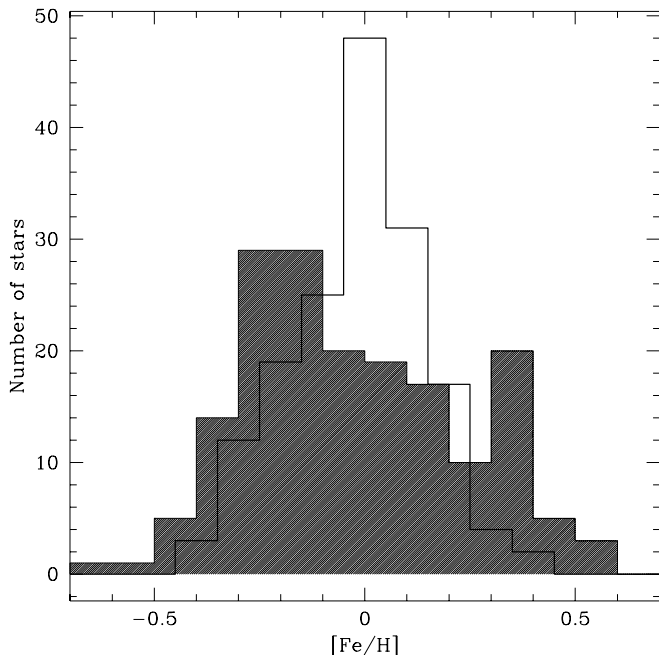

FIG. 11.—Histogram of [Fe/H] for stars more massive than 1.4 $M_\odot$. The thick line is the histogram for the observed stars while the light line histogram, which is also shaded, is the result of a Monte Carlo experiment in which a single Jupiter analogue was accreted onto 30% of the stars. The bimodal nature of the latter model arises because we have assumed that the planetary material, which contains 1.8 $M_\oplus$ of iron, is mixed with 3×10^{-3} $M_\odot$ of the outer layers of the star; this results in a large increase in the surface abundance of iron of those stars that accrete the planets. The mean metallicity of the entire sample has been forced to match the observed mean metallicity. The bimodal distribution of the Monte Carlo model is distinctly different from the observed distribution.

time. This would involve accreting the planets when the convection zone had a mass selected so as to dilute the iron by the proper amount. This strikes us as contrived, so we have not pursued the matter.

6.3. *Surface Metallicity Enhancement by Mass Loss or Dust Accretion*

The solar wind is observed to be iron rich; in fact, many elements with low first-ionization potentials are more abundant, while He, with its very high first-ionization potential, is underabundant (Meyer 1993; Geiss 1998). If a substantial portion of the stellar convection zone were lost in a massive wind, then the photospheric iron abundance would be less than the bulk abundance. If less massive stars suffer larger mass losses (relative to their more massive convection zones), this would produce a population in which less massive stars have lower metallicity than more massive stars, as we have found. When these low-mass stars evolve, deep convection zones will form and mix metal-rich material up to the surface; the high-mass stars will also show a slight increase in iron abundance.

However, what we appear to see is that as massive stars evolve, their metallicities decrease; we do not know what the low-mass stars do when they evolve. There is a second difficulty with this scenario. The mass loss rates required of low-mass stars are excessive; to lose a substantial fraction of the convection zone ($\sim 0.05\ M_\odot$ for a 0.8 $M_\odot$ star) the wind must carry away $\sim 5 \times 10^{-11}\ M_\odot\ \mathrm{yr}^{-1}$ for a billion years. The solar mass loss rate is $\sim 3 \times 10^{-14}\ M_\odot\ \mathrm{yr}^{-1}$. Recent limits on the mass-loss rates in K dwarfs are much lower, $10^{-12}\ M_\odot\ \mathrm{yr}^{-1}$ or less (Lim & White 1996; van den Oord & Doyle 1997).

Of course, the observation that lithium and beryllium depletions are correlated indicate that mass loss does not extend down to masses of order $3 \times 10^{-2}\ M_\odot$ in stars of mass ~ 1.2–$1.4\ M_\odot$. Taken together, these facts suggest that mass loss is not responsible for the metallicity variations we find.

Many young stars of roughly solar or larger mass show infrared excesses caused by circumstellar dust (Aumann et al. 1984; Habing et al. 1999; Decin et al. 2000). Much of this dust may end up on the star. Dust particles that absorb photons moving radially and then radiate them isotropically (in the dust rest frame) lose angular momentum in a process called the Poynting-Robertson effect. The amount of angular momentum lost ($\delta\ell$) per photon of frequency ν is $\delta\ell/\ell \sim h\nu/mc^2$, where m is the rest mass of the dust particle. Thus, for each accreted dust particle, a star must emit $\ell/\delta\ell$ photons, which means it must emit a total energy approximately equivalent to the rest mass energy of the accreted material. The total energy emitted during the period of dust accretion is larger than this by $1/\tau$, where τ is the optical depth to dust absorption. Thus, for a star radiating at approximately solar luminosity, the accretion of material will take a time

$$T_{\mathrm{dust}} \sim \frac{10^8\ \mathrm{yr}}{\tau} \left(\frac{M_{\mathrm{acc}}}{2\ M_\oplus}\right)\left(\frac{L_\odot}{L}\right). \tag{16}$$

For $\tau \sim 1$, this number corresponds roughly to the observed lifetime of dust around young massive (F) stars (Habing et al. 1999), but the spherically averaged τ is obviously considerably less than 1; values near 10^{-4} are typical.

Decin et al. (2000) find longer lived disks (~ 1 Gyr) of similar optical depth, but the maximum amount of dust that such stars can accrete is still much less than an Earth mass. We conclude that dust accretion is unlikely to provide enough material to explain the apparent iron enhancements we see.

6.4. Accretion of the Interstellar Medium

Observations of the interstellar medium in the vicinity of the Sun indicate that it has roughly solar abundances ($\sim +0.05$ dex) of some elements, such as Zn, P, and S (Howk, Savage, & Fabian 1999). Iron is typically depleted, probably onto dust grains. The youngest stars in our sample have [Fe/H] ≈ 0.2 (Fig. 3), slightly larger than the ISM, but our results indicate that about 0.05–0.1 of this is because of pollution. This is consistent with the notion that the bulk metallicity of young stars will equal that of the ISM out of which they form.

The implication is that older stars have metallicities lower than that of the ISM in which they currently reside. Accretion of the relatively metal-rich ISM material could in principle produce metallicity signatures of the type we have found. However, it seems that the youngest stars in our sample may be metal rich compared to the present day ISM. In view of the rather large errors in the metallicity determinations, we feel that this conclusion has to be considered as tentative.

6.5. β Pictoris

The star β Pic is surrounded by a dusty disk (Smith & Terrile 1984). The dust is believed to have a lifetime shorter than the estimated age of the star ($\lesssim 10^8$ yr) and so must be replenished, possibly by collisions between planetesimals (Lecavelier Des Etangs, Vidal-Madjar, & Ferlet 1996). Transient redshifted absorption features have been seen in spectra of β Pic for the last decade (Boggess et al. 1991; Lagrange et al. 1996). These events have been interpreted as infalling comets or asteroids. Events with very high velocities (> 100 km s^{-1}) are seen a few times per month (Beust et al. 1991; Beust & Morbidelli 2000). Similar transients are seen around numerous other young stars (de Winter et al. 1999; Grady et al. 1999).

The absorption features are believed to be produced by the cometary tails of the infalling bodies; Beust & Morbidelli argue that the infalling bodies must have radii larger than ~ 10 km in order to survive the evaporation long enough to evolve onto the inferred highly eccentric orbits. They estimate that 1.8–18 $M_\oplus$ of material is removed from the planetesimal disk by this process if it has continued for 10^8 yr. They refer to evaporation of these bodies; however, a small but substantial fraction of them will survive long enough to strike the star. This could provide enough material to give the signature we have seen.

6.6. Solar Pollution

The Sun is metal rich for stars of its age and mass, as can be seen from Figures 3 and 4. The implication is that the radiative interior of the Sun might have a metallicity slightly lower than the photosphere. A number of authors (Joss 1974; Christensen-Dalsgaard et al. 1979; Levy & Ruzmaikina 1994; Jeffery, Bailey, & Chambers 1997) suggested this possibility two decades ago as a way out of the solar neutrino problem; lowering the metallicity of the solar interior

reduces the radiative gradient, which, in turn, would lower the inferred temperature in the core. Finally, a lower core temperature would predict that fewer neutrinos would be emitted compared with that of the standard solar model.

The metallicity deficit required to explain the lack of solar neutrinos is much larger than the 0.017 dex increase resulting from the accretion of ~ 0.4 $M_\oplus$ of iron. This avenue for solving the neutrino problem was dropped by solar workers, partly for this reason. More recently, Henney & Ulrich (1998) examined polluted models to see if accurate measurements of the solar five minute oscillations (p-modes) could be used to detect differences between the metallicities of the surface convection zone and the radiative interior. They found that current data was unable to distinguish between unpolluted models and models with ~ 10 $M_\oplus$ of accreted cometary material. The effect on the production of solar neutrinos was also negligible.

As an aside, we note that the SOHO satellite has discovered a large number of Sun grazing comets, a class of comets that plunge into the Sun (see Raymond et al. 1998 and references therein). Roughly 200 have been observed by SOHO over its lifetime to date. Raymond et al. give an estimate of about 10^3 cm for the radius of the comet they observed. If most of the observed objects are of this size, and if we assume that the currently observed rate has been more or less steady over the lifetime of the Sun (one strikes the Sun roughly every day as observed in 2000), then the mass of accreted material would be about one one-millionth of an Earth mass. Note, however, that most of the comets seen by SOHO appear on dynamical grounds to be the result of the breakup of a single object, so that the currently observed flux is likely to be a burst of transient activity.

7. CONCLUSIONS

We analyzed some 640 stars from the Cayrel de Strobel catalog having spectroscopically determined metallicities and well-determined Hipparcos parallaxes. Using a large grid of stellar models, we determined the age and mass of the stars in our sample. We then examined the variation of metallicity with stellar age and mass.

We find clear evidence of a dependence of stellar metallicity with age (Fig. 6); younger stars are more metal rich, as expected from stellar nucleosynthesis. We also find that more massive stars are younger than less massive stars, as expected from the theory of stellar evolution (Fig. 7). From the previous two results, we expect to find that more massive stars are metal rich. We do see such a dependence of metallicity on stellar mass.

However, we have found striking variations from the prediction of the observed age-metallicity and age-mass relations. First, the slope of the metallicity-mass relation is larger than expected. Second, there appear to be variations from the predicted (roughly linear) relation between metallicity and mass. These variations in the photospheric iron abundances with stellar mass mimic the variations seen in lithium abundances in cluster stars. They are consistent with the accretion of an average of ~ 0.4–0.6 $M_\oplus$ of iron onto the surfaces of main-sequence stars.

It is very possible that the complicated abundance patterns we see arise from selection effects in the Cayrel de Strobel catalog. For example, requiring $B - V > 0.5$ (as in the Favata et al. sample mentioned in § 5.3) will produce a trend of increasing metallicity with stellar mass. The surest way to confirm or rule out this type of problem is to

produce a true volume-limited sample of stars with spectroscopic metallicities obtained in a uniform manner. Several hundred stars would be sufficient.

In the absence of such a sample, we resort to other tests of our result. If the abundance patterns we see are caused by pollution, then evolved stars, in which the mass of the surface mixing region has increased over the main-sequence value, will have lower average metallicities. We do find that the iron abundances of Hertzsprung gap stars are, on average, lower than those of main-sequence stars. It is not clear how a selection effect would produce such a difference between the apparent abundances of dwarfs and Hertzsprung gap stars since the fluxes, surface gravities, and effective temperatures of the two populations are nearly identical. We tentatively conclude that terrestrial-type material is common around solar-type stars in the solar neighborhood.

If we allow for the accretion of $\sim 0.5\ M_\oplus$ of iron, the apparent slope of the age-metallicity relation overestimates the true slope since the more massive stars tend to have surface mixing layers with smaller mass than those of less massive stars. (This trend is apparently reversed for stars between about 1.1 and 1.4 $M_\odot$; over this range, the more massive stars have larger surface mixing layers.) If this result holds for other samples, models of galactic chemical evolution will have to correct for pollution of the surface layers of stars. In our sample, the correction reduces the age-metallicity slope from -0.21 dex per log Gyr to -0.14, a 30% correction.

REFERENCES

Alexander, D. R., & Ferguson, J. W. 1994, ApJ, 437, 879
Aumann, H. H., et al. 1984, ApJ, 278, L23
Bahcall, J. N. 1989, Neutrino Astrophysics (Cambridge: Cambridge Univ. Press)
Bahcall, J. N., & Pinsonneault, M. H. 1995, Rev. Mod. Phys., 67, 781
Balachandran, S. 1995, ApJ, 446, 203
Beust, H., & Morbidelli, A. 2000, Icarus, 143, 170
Beust, H., Vidal-Madjar, A., Ferlet, R. & Lagrange-Henri, A. M. 1991, A&A, 241, 488
Boesgaard, A. 1991, ApJ, 370, L95
Boesgaard, A. M., & Tripicco, M. J. 1986, ApJ, 302, L49
Boggess, A., Bruhweiler, F. C., Grady, C. A., Ebbets, D. C., Kondo, Y., Trafton, L. M., Brandt, J. C. & Heap, S. R. 1991, ApJ, 377, L49
Butler, R. P., & Marcy, G. W. 1996, ApJ, 464, L153
Calvet, N. 1997, in IAU Symp. 182, Herbig-Haro Flows and the Birth of Stars, ed. B. Reipurth & C. Bertout (Dordrecht: Kluwer), 417
Cayrel de Strobel, G., Soubiran, C., Friel, E. D., Ralite, N. & Francois, P. 1997, A&AS, 124, 299
Chaboyer, B., Green, E. M., & Liebert, J. 1999, AJ, 117, 1360
Charbonnel, C., Vauclair, S., & Zahn, J.-P. 1992, A&A, 255, 191
Christensen-Dalsgaard, J., Gough, D. O., & Morgan, J. G. 1979, A&A, 73, 121
de Bruijne, J. H. J., Hoogerwerf, R., & de Zeeuw, P. T. 2000, ApJ, 544, L65
Decin, G., Dominik, C., Malfait, K., Mayor, M., & Waelkens, C. 2000, A&A, 357, 533
Deliyannis, C. P., Boesgaard, A. M., Stephens, A., King, J. R., Vogt, S. S., & Keane, M. J. 1998, ApJ, 498, L147
de Medeiros, J. R., & Mayor, M. 1999, A&AS, 139, 433
de Winter, D., Grady, C. A., van den Ancker, M. E., Pérez, M. R., & Eiroa, C. 1999, A&A, 343, 137
Edvardsson, B., Andersen, J., Gustafsson, B., Lambert, D. L., Nissen, P. E., & Tomkin, J. 1993, A&A, 275, 101
Favata, F., Micela, G., & Sciortino, S. 1997, A&A, 323, 809
Geiss, J. 1998, Space Sci. Rev., 85, 241
Gilroy, K. K. 1989, ApJ, 347, 835
Gladman, B. J., et al. 1997, Science, 277, 197
Gonzalez, G. 1997, MNRAS, 285, 403
Grady, C. A., Pérez, M. R., Bjorkman, K. S., & Massa, D. 1999, ApJ, 511, 925
Grevesse, N., & Anders, E. 1989, in AIP Conf. Proc. 183, Cosmic Abundances of Matter, ed. C. J. Waddington (New York: AIP), 1
Grevesse, N., & Noels, A. 1993, in Origin and Evolution of the Elements, ed. N. Prantzos, E. Vangioni-Flam, & M. Casse (Cambridge: Cambridge Univ. Press), 15
Guenther, D. B., Demarque, P., Kim, Y.-C., & Pinsonneault, M. H. 1992, ApJ, 387, 372
Guillot, T. 1999a, Science, 286, 72
Guillot, T. 1999b, Planet. Space Sci., 47, 1183
Gullbring, E., Calvet, N., Muzerolle, J., & Hartmann, L. 2000, ApJ, 544, 927
Gustafsson, B., Karlsson, T., Olsson, E., Edvardsson, B., & Ryde, N. 1999, A&A, 342, 426
Habing, H. J., et al. 1999, Nature, 401, 456
Henney, C. J., & Ulrich, R. 1998, in Structure and Dynamics of the Interior of the Sun and Sun-like Stars, ed. S. Karzennik & A. Wilson (Noordwijk: ESA), 473
Holman, M., & Murray, N. 1996, AJ, 112, 1278
Howk, J. C., Savage, B. D., & Fabian, D. 1999, ApJ, 525, 253
Hubbard, W. B., Pearl, J. C., Podolak, M., & Stevenson, D. J. 1995, in Neptune and Triton, ed. D. P. Cruikshank (Tucson: Univ. of Arizona Press), 109
Iglesias, C. A., & Rogers, F. 1996, ApJ, 464, 943
Jeffery, C. S., Bailey, M. E., & Chambers, J. E. 1997, The Observatory, 117, 224
Jones, B. F., Fischer, D., & Soderblom, D. R. 1999, AJ, 117, 330
Joss, P. C. 1974, ApJ, 191, 771
Kirkwood, D. 1867, Meteoric Astronomy: A Treatise on Shooting-Stars, Fireballs, and Aerolites (Philadelphia: Lippincott)
Konigl, A., & Pudritz, R. E. 2000, in Protostars and Planets IV, ed. V. Mannings, A. P. Boss, & S. S. Russell (Tucson: Univ. of Arizona Press), 759
Kurucz, R. L. 1993, CD-ROM 13, ATLAS9 Stellar Atmosphere Programs and 2 km/s Grid (Cambridge: SAO)
Lagrange, A., et al. 1996, A&A, 310, 547
Laughlin, G. 2001, ApJ, 545, 1064
Laughlin, G., & Adams, F. C. 1997, ApJ, 491, L51
Lecavelier Des Etangs, A., Vidal-Madjar, A., & Ferlet, R. 1996, A&A, 307, 542
Levy, E. H., & Ruzmaikina, T. V. 1994, ApJ, 431, 881
Lim, J., & White, S. M. 1996, ApJ, 462, L91
Lin, D. N. C. 1997, in ASP Conf. Ser. 121, Accretion Phenomena and Related Outflows, ed. D. Wickramasinge, B. V. Bicknell, & L. Ferrario (San Francisco: ASP), 321
Liou, J. C., & Malhotra, R. 1997, Science, 275, 93
Longhi, J., Knittle, E., Holloway, J. R., & Wänke, H. 1992, in Mars (Tucson: Univ. of Arizona), 184
Marcy, G. W., & Butler, R. P. 1996, ApJ, 464, L147
Marcy, G. W., Cochran, W. D., & Mayor, M. 2000, in Protostars and Planets IV, ed. V. Mannings, A. P. Boss, & S. S. Russell (Tucson: Univ. of Arizona Press), 1285
Mathioudakis, M., Fruscione, A., Drake, J. J., McDonald, K., Bowyer, S., & Malina, R. F. 1995, A&A, 300, 775
Mayor, M., & Queloz, D. 1995, Nature, 378, 355
Meusinger, H., Reimann, H.-G., & Stecklum, B. 1991, A&A, 245, 57
Meyer, J.-P. 1993, in Origin and Evolution of the Elements, ed. N. Prantzos, E. Vangioni-Flam, & M. Casse (Cambridge: Cambridge Univ. Press), 26
Michaud, G., & Proffitt, C. R. 1993, in IAU Colloq. 137, Inside the Stars, ed. A. Baglin & W. W. Weiss (San Francisco: ASP), 246
Murray, N., & Chaboyer, B. 2001, ApJ, submitted
Muzerolle, J., Calvet, N., & Hartmann, L. 1998, ApJ, 492, 743
Olive, K., Steigman, G., & Skillman, E. D. 1997, ApJ, 483, 788
Petit, J.-M., Morbidelli, A., & Valsecchi, G. B. 1991, Icarus, 141, 367
Podolak, M., Hubbard, W. B., & Stevenson, D. J. 1991, in Uranus, ed. J. T. Bergstralh, E. D. Miner, & M. Matthews (Tucson: Univ. of Arizona), 29
Raymond, J. C., et al. 1998, ApJ, 508, 410
Richer, J. S., Shepherd, D. S., Cabrit, S., Bachiller, R., & Churchwell, E. 2000, in Protostars and Planets IV, ed. V. Mannings, A. P. Boss, & S. S. Russell (Tucson: Univ. of Arizona Press), 867
Santos, D., Israelian, G., & Mayor, M. 2000, A&A, 363, 228
Shu, F. H., Najita, J. R., Shang, H., & Li, Z. 2000, in Protostars and Planets IV, ed. V. Mannings, A. P. Boss, & S. S. Russell (Tucson: Univ. of Arizona Press), p. 789
Smith, B., & Terrile, R. 1984, Science, 226, 1421

Soderblom D. R., Jones B. F., Balachandran S., Stauffer J. R., Duncan D. K., Fedele S. B., & Hudon J. D. 1993, AJ, 106, 1059
Talon, S., & Charbonnel, C. 1998, A&A, 335, 959
van den Oord, G. H. J., & Doyle, J. G. 1997, A&A, 319, 578
Vauclair, S. 1991, in IAU Symp. 145, Evolution of Stars: The Photospheric Abundance Connection, ed. G. Michaud, A. Tutukov, & M. Bergevin (Dordrecht: Kluwer), 327

Weidenschilling, S. J. 1977, Ap&SS, 51, 153
Wetherill, G. 1992, Icarus, 100, 307
Wisdom, J. 1983, Icarus, 56, 51
Wolszczan, A., & Frail, D. A. 1992, Nature, 355, 145